Parasitology

cambridge.org/par

Insights on the morphological aspects of lipid accumulation and excretion in adult *Caryophyllaeus brachycollis* (Cestoda, Caryophyllidea)

Larisa Poddubnaya[1], Massimo Lorenzoni[2], Galina I. Izvekova[1], Antonella Carosi[2] and Bahram Sayyaf Dezfuli[3]

[1]Papanin Institute for Biology of Inland Waters, Russian Academy of Sciences, Borok, Yaroslavl District, Russia; [2]Department of Chemistry, Biology and Biotechnology, University of Perugia, Perugia, Italy and [3]Department of Life Sciences & Biotechnology, University of Ferrara, Ferrara, Italy

Research Article

Cite this article: Poddubnaya L, Lorenzoni M, Izvekova GI, Carosi A, Sayyaf Dezfuli B (2026) Insights on the morphological aspects of lipid accumulation and excretion in adult *Caryophyllaeus brachycollis* (Cestoda, Caryophyllidea). *Parasitology* **153**, 774–783. https://doi.org/10.1017/S0031182026101930

Received: 13 November 2025
Revised: 27 March 2026
Accepted: 27 March 2026
First published online: 15 April 2026

Keywords:
excretory bladder; lipid droplets; lipid excretion; storage myocytes; tegument

Corresponding author:
Bahram Sayyaf Dezfuli;
Email: dzb@unife.it

Abstract

This is the first ultrastructural study of an adult tapeworm providing data on the morphological aspects of the pathways of lipid excretion via the tegumental surface and excretory system in the monozoic tapeworm *Caryophyllaeus brachycollis* (Janiszewska, 1953) from the chub *Squalius tenellus* (Heckel, 1843) obtained from a lake in the Bosnia-Herzegovina Federation. Our study has shown that the release of lipid droplets onto the parasite–host interface from the tegumental cytoplasm is carried out with the participation of tegumental vesicles, which clustered and fused with each other to form electron-lucent, membrane-bound sacs around lipid droplets. The ultrastructural pattern of the excretory bladder is presented for the first time for an adult tapeworm. In *C. brachycollis*, the syncytial epithelial lining of both the distal and proximal bladder is a derivative of the tegumental distal cytoplasm of the posterior body surface. Variations in the structural organization of both bladder parts were observed in the kinds of luminal microtriches and in the presence of large cytoplasmic protrusions in the proximal bladder. In *C. brachycollis*, the lipid droplets are released into the proximal bladder lumen via 10 collecting descending excretory ducts. In adult mature monozoic caryophyllidean tapeworms, an accumulation of a large number of sarcoplasmic lipid droplets is observed and their presence in the protonephridial cyrtocytes is revealed at the posterior body end, where there are the reproductive organs and ducts.

Introduction

Lipids are a diverse group of compounds that play essential roles in cell structure and are the main components of cell membranes (Alvite and Esteves, 2012; Hashimoto and Hossain, 2018). Studies of cestode lipids have revealed the presence of these substances in the intestines of their hosts, with the highest amounts found in tapeworms (Humbe et al., 2011; Khawal et al., 2020; Saraf and Katyayani, 2020; Bhogil et al., 2022; Phadke, 2024). There is a close relationship between the fatty acid composition of the host animal and its parasites (Jawale et al., 2011; Mondal et al., 2016; Yuskiv and Yuskiv, 2020). The lipid content in cestodes varies from 7.5 to 37.3% of total body weight (Smyth and McManus, 1989; Biswal et al., 2014). Over 500 putative metabolites, including lipids, have been reported in tapeworm species (Wangchuk et al., 2019; Yeshi et al., 2022). Lipids, including glycerol and several fatty acids, have been found in the excretory secretory products of tapeworms (Ritler et al., 2019; Wangchuk et al., 2019; Wangckuk et al., 2023). The utilization of lipids by helminths varies across different life cycle stages (Soprunov, 1987; Conn, 1993; Moczoń, 2006) and many lipids found in adult worms are stored and excreted (Wangckuk et al., 2023).

The ultrastructure of various tapeworm cell components reported over the past 40 years has shown that the storage myocytes of adult cestodes accumulate numerous lipid droplets (Conn, 1993; Moczoń, 2006) as well as mature vitellocytes and the eggs store lipid droplets in most cestode species (Świderski and Xylander, 2000; Młocicki et al., 2010; Biswal et al., 2014). Regarding monozoic caryophyllidean tapeworms, lipid droplets are present in the cytoplasm of their tegumental cells, including their so-called scolex tegumental glands (Richards and Arme, 1981; Sayyaf Dezfuli et al., 2024). The presence of lipid droplets has also been revealed in the lumen of the excretory ducts of caryophyllidean cestodes (Poddubnaya, 2003). In the vitellocyte cytoplasm of most caryophyllidean cestodes, lipid droplets were not observed (Świderski and Mackiewicz, 1976; Świderski et al., 2004, 2009); however, in some of these worms, there were a few lipid droplets in their vitellocytes and eggs (Bruňanaská et al., 2012).

© The Author(s), 2026. Published by Cambridge University Press. This is an Open Access article, distributed under the terms of the Creative Commons Attribution licence (http://creativecommons.org/licenses/by/4.0), which permits unrestricted re-use, distribution and reproduction, provided the original article is properly cited.

The present study is the first detailed ultrastructural investigation on the accumulation and excretion of lipid droplets in the adult caryophyllidean monozoic cestode *Caryophyllaeus brachycollis* (Janiszewska, 1953) from the host chub, *Squalius tenellus* Heckel, 1843. This study aimed to document the presence of lipid droplets in the tegumental, muscle and excretory cell components, providing data on the morphological aspects of the pathways of their excretion via the tegumental surface and excretory system. The study provides a first account of the ultrastructure of the excretory bladder of an adult tapeworm.

Materials and methods

A sub-population of 22 specimens of chub *Squalius tenellus* was collected in July 2023 from Lake Blidinje in Blidinje Natural Park in Southern Bosnia-Herzegovina Federation (43°36′25′′N, 17°29′48′′E) using gill nets. In the field, chubs were anaesthetized using MS222 (125 mg L^{-1}, tricaine methanesulfonate; Sandoz, Basel, Switzerland), then the spinal cords were severed and fish were dissected ventrally. The body cavity and visceral organs were visually inspected, and the alimentary canal was removed and opened longitudinally to search for parasites. Pieces of infected intestines with attached worms measuring up to 18 × 18 mm in size were excised and fixed in 10% neutral buffered formalin for 36 h. Then, the samples were dehydrated through an alcohol series and then paraffin wax-embedded using a Shandon Citadel 2000 tissue processor. Multiple 5 µm sections were taken from each tissue block, stained with Alcian Blue/PAS, Haematoxylin and Eosin, and Giemsa and examined and photographed using a Nikon Microscope ECLIPSE 80i. Multiple histological sections were obtained from each tissue block and examined and photographed under an optical microscope (Nikon Eclipse 80i; Nikon, Tokyo, Japan). For the excretory bladder study, 28 worms free in the intestinal lumen were fixed in 10% neutral buffered formalin for 36 h. After dehydration, the samples were embedded in paraffin as described above, sectioned, stained with Alcian Blue/PAS and Giemsa, and then photographed using optical stereomicroscope (Nikon SMZ800 with software Nis Elements, Tokyo, Japan).

For scanning electron microscopy, 10 specimens of *C. brachycollis* fixed alive in 5% glutaraldehyde in 0.1 M sodium cacodylate buffer (pH 7.2) were dehydrated in a graded ethanol series with a final change to absolute acetone. After dehydration, specimens were critical-point dried and desiccated using an HCP-2 critical-point dryer (Hitachi, Tokyo, Japan). Later, dried specimens were mounted on stubs, sputter-coated using a JFC 1600 Auto Fine Coater (JEOL Ltd, Tokyo, Japan) with gold–palladium (15–20 µm in thickness) and examined using a JEOL-JSM-6510LV microscope (JEOL Ltd, Tokyo, Japan) at 15 kV.

For transmission electron microscopy, over 40 isolated *C. brachycollis* specimens were fixed in the field in 5% glutaraldehyde in 0.1 M sodium cacodylate buffer (pH 7.2) for 5 h at 5 °C, rinsed twice for 20 min in the same buffer and post-fixed in 1% osmium tetroxide for 1 h. Fixed specimens were dehydrated in a graded ethanol series with a final change to absolute acetone and embedded in a mixture of Araldite and Epon using the instructions provided with the Araldite/Embed-812 EM Embedding Kit (Sigma-Aldrich, Buenos Aires, Argentina). Ultrathin sections (50–90 nm in thickness) were cut on a Leica MZ6 ultramicrotome (Leica Microsystems, Wetzlar, Germany), mounted on formvar-coated copper and stained in uranyl acetate and lead citrate before examination with a JEOL JEM 1011 microscope (JEOL Ltd, Tokyo, Japan) at 80 kV.

Results

The occurrence of lipid droplets in adult C. brachycollis

The body surface of *C. brachycollis* is lined with a syncytial tegumental layer (distal tegumental cytoplasm), which rests on a basal matrix and is connected to sunken perinuclear cell bodies (tegumental perikarya) via tegumental cytoplasmic processes (Figures 1A, 3A, 3G). In *C. brachycollis*, the tegumental perikarya of the scolex are specialized to produce both elongated secretory granules and the tegumental structured bodies, dense bodies and electron-lucent vesicles, as well as glycogen and moderately dense lipid droplets (0.5–1.3 µm in diameter) are present in their cytoplasm (Figures 2A and D, 3C and F). The tegumental cells of the middle and posterior body produce heterogeneous vesicles with dense internal coating and significant amounts of moderately dense lipid droplets (0.5–2.0 µm in diameter) (Figures 2E and G, 3H and K). The lipid droplets, together with secretory granules and tegumental bodies (in the scolex region) (Figure 3A and C, F) or together with tegumental heterogeneous vesicles (in the rest of the body) (Figure 3G–L), passed into the distal tegumental cytoplasm (Figure 3A).

A large area between the different cell components of the body of adult *C. brachycollis* was occupied by pseudopodia-like sarcoplasmic processes of storage myocytes containing a glycogen-rich cytoplasm jumbled with a number of lipid droplets (Figure 2B and C, F). Individual moderately dense sarcoplasmic lipid droplets are of various sizes (0.4–1.1 µm in diameter) and irregular outlines (Figure 2B and C). The myocyte perikarya were situated in the medullary parenchyma and included the nucleus and a narrow, dense zone of the perinuclear cytoplasm filled with ribosomes (Figure 2B). In the mature worms, at the posterior body portion, lipid droplets are prevalent in the sarcoplasmic processes and coalesce to form single large lipid droplets that may reach up to 11 µm in diameter (Figure 2F). The sarcoplasmic processes were interdigitated with each other (Figure 2J and K). Close rapprochement of excretory ducts and sarcoplasmic processes of storage muscle cells was observed (Figure 2J, K and I).

The excretory system of *C. brachycollis* comprises terminal cells (cyrtocytes), a network of ducts and an excretory bladder with an excretory pore at the posterior body end. Each cyrtocyte consists of a combination of 2 cells, the processes of which interdigitate to form a weir, a filtering apparatus, where the filtration and transport of nutrients and metabolites from the parenchyma to the excretory ducts takes place. In TEM sections of 50–90 nm thick, more than 50 cilia were observed in each tuft of *C. brachycollis* (Figure 2H and I). The ciliary tuft was surrounded by a cytoplasmic cord formed by proximal duct cell (Figure 2H and I). In adult *C. brachycollis*, irregularly shaped lipid droplets were observed in the area between the ciliary tuft and the cytoplasmic cord of a number of cyrtocytes in the posterior portion of the cestode's body (Figure 2H and I).

The epithelium of the excretory ducts consisted of a syncytial cytoplasmic layer on an extracellular matrix with nucleated bodies below it (Figure 2L–N). The luminal plasma membrane of the excretory ducts was thrown into thin, irregular and laminated cytoplasmic extensions (Figure 2L and N). The basal plasma membrane of the duct epithelium was increased by deep infolding, which penetrated the epithelial cytoplasm (Figure 2M and N). The cytoplasmic matrix contained small, rounded vesicles, many of which contained electron-dense contents, and mitochondria, glycogen particles and lipid droplets were observed in the epithelial cytoplasm (Figure 2M and N). The lumen of the collecting ducts contained moderately dense lipid droplets (Figure 2L and M).

https://doi.org/10.1017/S0031182026101930 Published online by Cambridge University Press

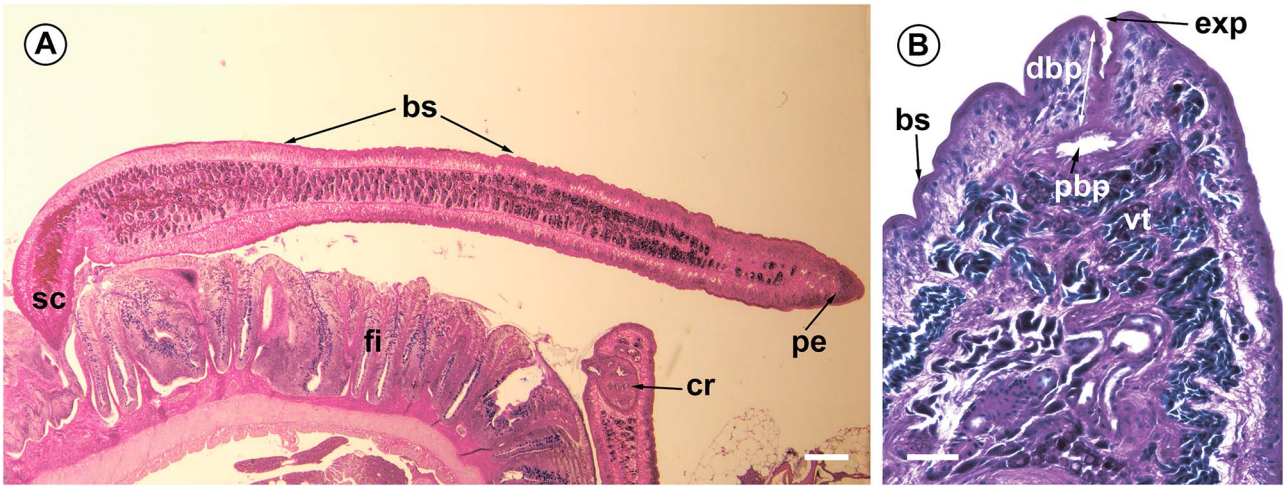

Figure 1. Histological sections of *C. brachycollis*. (A) Histological section of the chub intestine showing an adult specimen with the scolex within the intestinal folds, stained with Alcian Blue/PAS. Scale bar = 300 μm. (B) Giemsa staining of a section of the posterior end; note the excretory bladder. Scale bar = 50 μm. Abbreviations: bs, body surface; cr, cirrus; dbp, distal bladder portion; exp, excretory pore; fi, fish intestine; pe, posterior end of worm's body; pbp, proximal bladder portion; sc, scolex; vt, vitelline follicles.

Release of lipid droplets onto the parasite–host interface through the distal tegumental cytoplasm of C. brachycollis

Moderately dense lipid droplets were observed along the thickness of the distal tegumental cytoplasm throughout the worm body, and these droplets were present at the host–parasite interface close to the worm surface (Figure 3A–D and G). Our results indicated that within the syncytial tegumental cytoplasm around the lipid droplets, electron-lucent vesicles clustered and fused with each other (Figure 3F and I, K, L). In some sections, lipid droplets were visible inside the membrane-bound electron-lucent sacs (Figure 3F, I, K and L). The sacs with lipid droplets were released from the body (Figure 3D, E and G). This may explain the presence of empty membrane-bound sacs and lipid droplets outside the body (Figure 3G). Moreover, along the middle part of the body surface, small surface cytoplasmic protrusions with tegumental bodies and lipid droplets were observed, with subsequent separation from the body surface (Figure 3H). In some photographs, the closely rapprochement of individual lipid droplets and microthrix surface was revealed (Figure 3B, F and J).

Cytoarchitecture of the excretory bladder of C. brachycollis

Besides the body tegument, lipid excretion is accomplished by the excretory system (Figures 2H–N and 4, 5). In *C. brachycollis*, the posterior-terminal excretory pore leads into the distal bladder duct (about 130 μm in length), which enlarges to form the bladder expansion of about 85 μm in diameter in its proximal portion (Figures 1B and 4A, B). The syncytial epithelial lining of the distal portion of the excretory bladder had the same ultrastructural characteristics as the distal tegumental cytoplasm of the posterior body tegument (Figure 4B and C). It was characterized by the presence of the same type of filamentous microtriches along its luminal surface and the presence of the same cytoplasmic inclusions in the syncytial distal cytoplasm, including lipid droplets (Figure 4C). Here, the bladder epithelium measured about 2.0–5.5 μm in thickness, the microthrix base was 0.7–1.0 μm in length and approximately 0.1 μm in diameter, and the tapering electron-dense caps were 0.4–0.5 μm in length (Figure 4C). The basal plasma membrane was supported by the extracellular matrix and formed large basal invaginations (Figure 4C). Muscle fibres extended along the entire bladder wall (Figure 4D and E). Lipid droplets were observed in the bladder lumen (Figures 4D, H and I, 5B). The folded epithelial syncytial lining of the proximal bladder portion varied in thickness from 1.5 to 7.0 μm (Figure 4D and E). The epithelial cytoplasm contained numerous small electron-lucent, moderately dense and dense vesicles (Figure 4F and H). Vesicles were often observed close to the luminal plasma membrane, and morphological evidence suggested that they were secreted into the lumen (Figure 4H and I). Several membrane-bound vesicles were also observed in the microtrichial space (Figure 4H). The luminal plasma membrane of the proximal bladder was elevated by large cytoplasmic protrusions of different sizes and shapes that protruded into the bladder lumen, including at their final stage where they are released into the bladder lumen (Figures 4E and G, 5B). Their cytoplasm often contained ovoid areas of sparse, heterogeneous content, where lipid droplets may be present (Figures 4G and 5B). The luminal surface of the proximal bladder portion was thrown up into abundant microtriches up to 4 μm in length (Figure 4E and F, I). The microthrix base measured between 0.5 and 0.7 μm in length and 0.1 μm in diameter; the microthrix cap measures from 1.5 to 3.5 μm in length. The inner core of the microthrix cap may contain electron-dense or electron-lucent components (Figure 4F and I). The bladder lumen contained large lipid droplets that increased in size when fused with one another (Figure 4D and G, H). The bladder was lined by a syncytium, the cell bodies of which were located underneath the basal matrix and the perinuclear cytoplasm contained numerous lipid droplets (Figure 4J). These lipid droplets passed into the bladder epithelial cytoplasm via cell cytoplasmic processes and were subsequently released through the bladder epithelium into the bladder lumen (Figure 4D and G–I). Within the bladder lumen, lipid droplets were observed close to the luminal surface, in the microtrichial space (Figure 4G and insert, I). In addition, the bladder epithelial cytoplasm contains lipid droplets that appear to be discharged into the bladder lumen via apocrine secretion. This occurs when lipid droplets accumulate in the protrusions of the proximal bladder epithelium (Figures 4G and 5B). Isolated protrusions were observed in the lumen of the bladder

https://doi.org/10.1017/S0031182026101930 Published online by Cambridge University Press

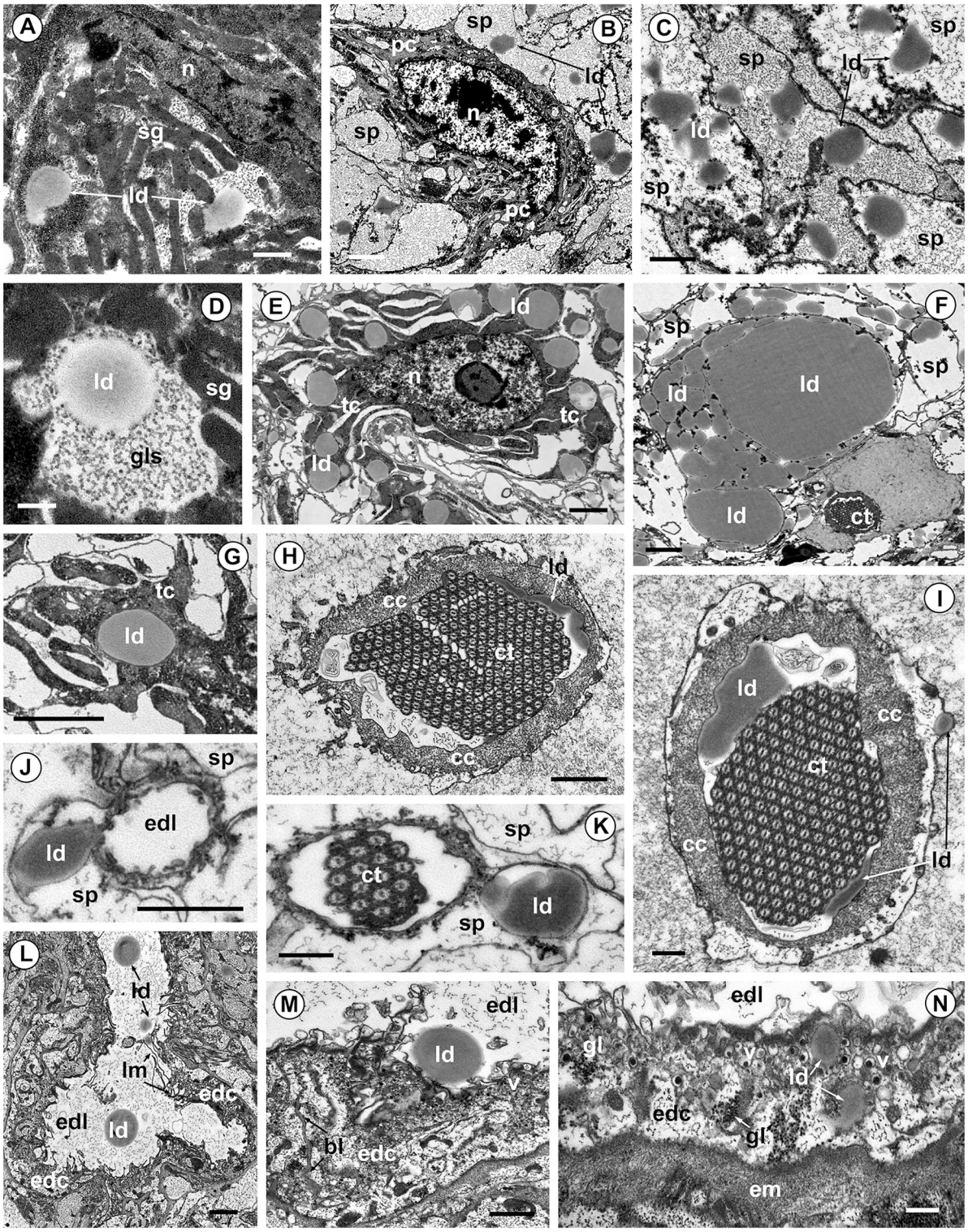

Figure 2. Occurrence of lipid droplets in adult *C. brachycollis*. (A, D) Scolex tegumental glandular cell cytoplasm with lipid droplets and secretory granules; note lipid droplets confined to the glycogen storage sites. Scale bars A = 0.5 μm, D = 0.2 μm. (B) Perikarya of the storage myocyte; note the dense perinuclear cytoplasm and numerous sarcoplasmic processes. Scale bar = 2 μm. (C) Tightly packed sarcoplasmic processes with lipid droplets. Scale bar = 1 μm. (E, G) Tegumental cell of the posterior body region; note a number of lipid droplets in the cytoplasm. Scale bar = 2 μm. (F) Sarcoplasmic processes filled with large lipid droplets in the posterior end of the mature worm. Scale bar = 2 μm. (H, I) Sections of ciliary tuft showing the presence of irregularly shaped lipid droplets between the ciliary tuft and cytoplasmic cord in cyrtocytes of the posterior body. Scale bar H = 1 μm, I = 0.5 μm. (J) Small excretory duct surrounded by sarcoplasmic processes, with a lipid droplet close to the duct epithelium. Scale bar = 1 μm. (K) Section through the proximal portion of the ciliary tuft surrounded by sarcoplasmic processes, containing a lipid droplet. Scale bar = 0.5 μm. (L) Collecting excretory duct, containing lipid droplets within the lumen. Scale bar = 1 μm. (M, N) Epithelial cytoplasm of the excretory collecting ducts, containing lipid droplets in the cytoplasmic lining and within the lumen of the excretory duct. Scale bar = 1 μm. Abbreviations: bi, basal invagination; cc, cytoplasmic cord surrounded ciliary tuft; ct, ciliary tuft; edc, excretory duct cytoplasm; edl, excretory duct lumen; em, extracellular basal matrix; gl, glycogen; gls, glycogen storage site; lm, luminal lamellae of collecting excretory duct; ld, lipid droplet; n, nucleus; pc, perinuclear cytoplasm; sg, secretory granules; sp, sarcoplasmic processes; tc, tegumental cytoplasm; v, vesicles.

https://doi.org/10.1017/S0031182026101930 Published online by Cambridge University Press

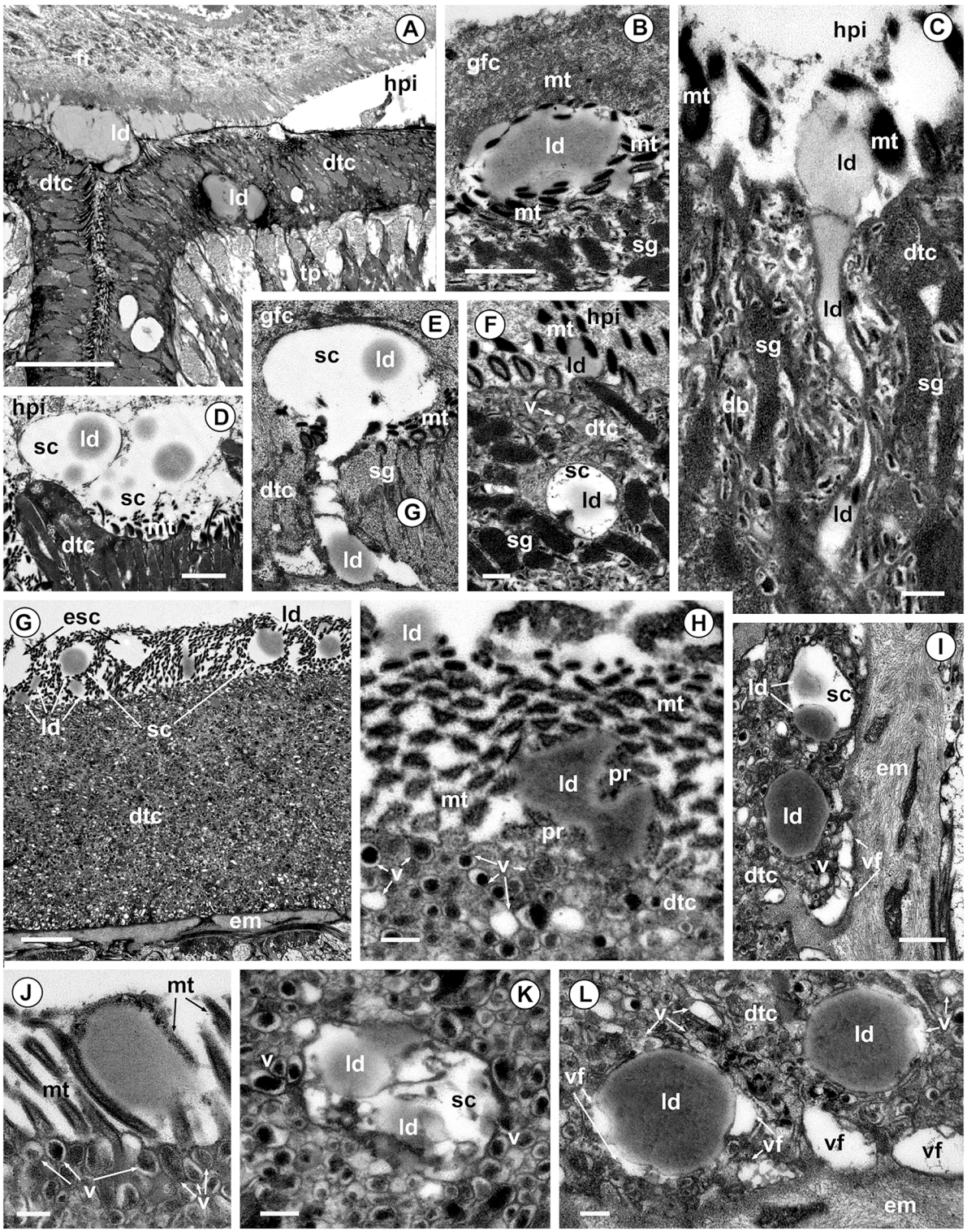

Figure 3. The release of lipid droplets through the distal tegumental cytoplasm in adult *C. brachycollis*. (A) Scolex region showing lipid droplets within tegumental lining and beyond it, at the interface of the worm's surface and the intestinal tract of the fish. Scale bar = 5 μm. (B) Lipid droplet in contact with microtriches of the apical scolex. Scale bar = 0.5 μm. (C) Release of a lipid droplet at the host–parasite interface; note the lipid droplet in contact with microtriches. Scale bar = 0.2 μm. (D) Two membrane-bound sacs with lipid droplets beyond the body surface. Scale bar = 1 μm. (E) Release of a membrane-bound sac containing a lipid droplet at the host–parasite interface. Scale bar = 0.5 μm. (F) Scolex distal tegumental cytoplasm showing a membrane-bound sac with a lipid droplet. Scale bar = 0.2 μm. (G) Membrane-bound sacs with 1 lipid droplet at the microthrix border of the middle body part showing empty sacs. Scale bar = 2 μm. (H) Protrusion of the tegumental surface of the posterior body part containing lipid droplets, showing numerous cytoplasmic vesicles of differing in content. Scale bar = 0.2 μm. (I, L) Posterior body showing tegumental cytoplasm. Note the membrane-bound sac with lipid droplets, close to individual lipid droplets where vesicle fusion occurs. Scale bars I = 0.5 μm, L = 0.2 μm. (J) Lipid droplet in contact with microtriches in the middle body, showing exocytotic vesicles near the plasma membrane. Scale bar = 0.2 μm. (K) A membrane-bound sac with lipid droplets in the tegumental cytoplasm of the middle body. Scale bar = 0.2 μm. Abbreviations: db, dense bodies; dtc, distal tegumental cytoplasm; em, extracellular basal matrix; esc, empty sac; gfc, glandular fibrillar content; hpi, host–parasite interface; ld, lipid droplet; sg, secretory granules; mt, microtriches; pr, protrusion of the body surface; sc, membrane-bound sac; tp, processes of the tegumental cells; v, vesicles; vf, vesicle fusion.

https://doi.org/10.1017/S0031182026101930 Published online by Cambridge University Press

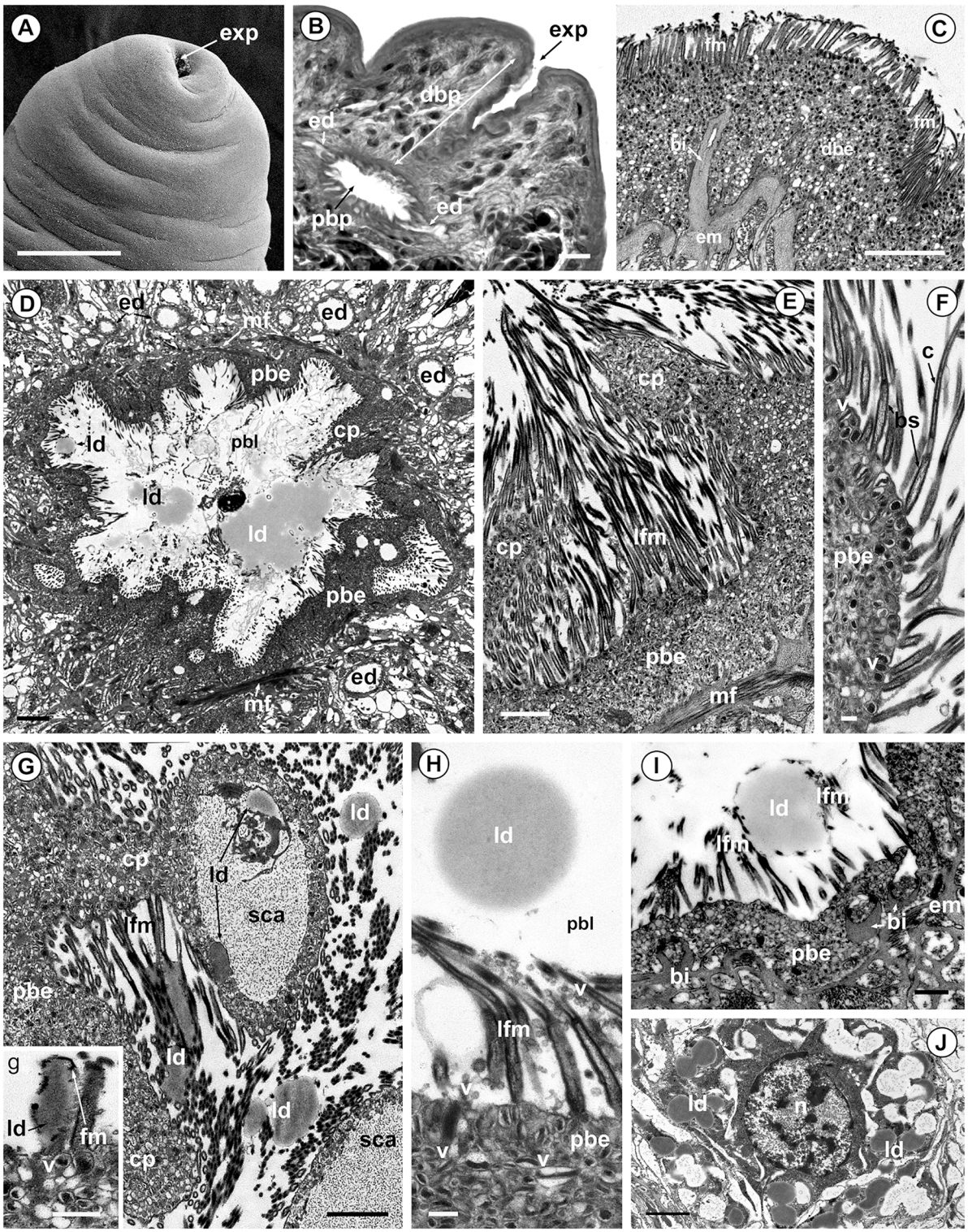

Figure 4. Ultrastructure of the excretory bladder of *C. brachycollis*. (A) Scanning electron microscopy view of the posterior end showing the terminal excretory pore. Scale bar = 100 µm. (B) Light microscopy section through excretory bladder showing the long distal bladder duct and its enlarged proximal portion. Scale bar = 30 µm. (C) Syncytial epithelial lining of the distal bladder portion showing deep basal invagination. Scale bar = 2 µm. (D) Enlarged proximal bladder portion showing lipid droplets within the bladder lumen and excretory ducts surrounding the proximal bladder portion. Scale bar = 2 µm. (E) Proximal bladder epithelium bearing long filamentous microtriches. Scale bar = 1 µm. (F) Long filamentous microtriches showing the electron-lucent content of their cap. Scale bar = 0.2 µm. (G) Proximal bladder epithelium showing sparse cytoplasm with lipid droplets and lipid droplets within the lumen. Scale bar = 1 µm. Insert (g) Discharge lipid droplet surrounded by microtriches. Scale bar = 0.2 µm. (H) Proximal bladder epithelium showing numerous vesicles close to its luminal surface and a number of vesicles within the space between microtriches. Scale bar = 0.2 µm. (I) Luminal lipid droplet surrounded by microtriches showing a number of unusual basal invaginations. Scale bar = 0.5 µm. (J) Bladder sunken cell body showing numerous lipid droplets in the perinuclear cytoplasm. Scale bar = 2 µm. Abbreviations: bi, basal invagination; bs, microthrix base; c, microthrix cap; cp, cytoplasmic protrusion; dbe, distal bladder epithelium; dbp, distal bladder portion; ed, excretory duct; em, extracellular basal matrix; exp, excretory pore; fm, filamentous microtriches; ld, lipid droplets; lfm, long filamentous microtriches; mf, muscle fibres; n, nucleus; pbe, proximal bladder epithelium; pbl, proximal bladder lumen; pbp, proximal bladder portion; sca, sparse cytoplasmic area; v, vesicles.

https://doi.org/10.1017/S0031182026101930 Published online by Cambridge University Press

(Figure 4D and H). These protrusions entered the bladder lumen by separating from the epithelial lining (Figure 5B).

Release of lipid droplets by the excretory ducts into the proximal bladder lumen of C. brachycollis

Our investigation supports the presence of 10 descending ducts in *C. brachycollis*, which are situated around the proximal excretory bladder (Figures 4D, 5A–C and E). The plasma membranes of the excretory bladder epithelium and the distal portions of the descending ducts are interconnected by septate junctions at the site where they are in contact (Figure 5). The descending excretory ducts contain lipid droplets in their lumen, which are passed into the bladder lumen (Figure 5). Lipid droplets are released from the excretory bladder pore in adult *C. brachycollis* (Figure 5A, B and E).

Discussion

Dynamics in lipid accumulation of parasitic worms

The monozoic caryophyllidean tapeworm, *C. brachycollis*, has a dixenic life cycle, with oligochaetes typically serving as intermediate hosts (procercoid stage of development), whereas adult worms are intestinal parasites of Cypriniformes, the chub *Squalius tenellus*. In adult *C. brachycollis*, moderately dense lipid droplets were observed in the cytoplasm of tegumental cells, including scolex glandular tegumental cells, in the sarcoplasmic processes of storage muscle cells, in the cyrtocytes and in the epithelial lining of the excretory ducts and excretory bladder, including within their lumen.

It is known that carbohydrates are an essential energy source for all adult parasitic helminths (Komuniecki and Harris, 1995). A common feature of most tapeworms is carbohydrate storage and lipid droplet deposition in myocytes (Conn, 1993). Stored glycogen is the most dominant form of carbohydrate in tapeworms and is the primary source of energy (Smyth and McManus, 1989). Glycogen concentration in tapeworms depends on their location inside the host, stage of parasite development and degree of adult maturity (Conn and Etges, 1984; Soprunov, 1987; Conn and Rocco, 1989; Smyth and McManus, 1989; Izvekova, 1997; Nanware et al., 2012). In adult tapeworms, lipid concentration increases gradually with worm maturation (Soprunov, 1987; Conn, 1993; Moczoń, 2006). In mature tapeworms with eggs, glycogen is absent in the sarcoplasmic processes, which are filled with lipid droplets (Biswal et al., 2014). As shown herein, in mature monozoic *C. brachycollis,* in the sarcoplasmic processes of storage myocytes at the posterior end of the body, where the reproductive organs and ducts are situated, there is an accumulation of a large number of lipid droplets, and often single droplets merge together to form larger droplets.

Interestingly, both caryophyllidean procercoids and progenetic caryophyllidean species, such as *Archigetes sieboldi*, inhabit the oligochaete coelom, and the sarcoplasmic processes of the early stage of procercoid development are filled with glycogen (Poddubnaya, 1995), while as the procercoids grow, the number of lipid droplets present increases (Poddubnaya et al., 2003). In digeneans, a large accumulation of lipids was observed in the adult *Leucochloridiamorpha lutea*, an intestinal parasite of birds (Shultz and Gvozdev, 1972). However, in the larval metacercarial stage of *L. lutea*, which was encountered just below the shells of a clam, *Viviparus* spp., the sarcoplasmic processes contained glycogen. Based on the above evidence, it is reasonable to presume that the lipid content varies at different stages of the life cycle of parasitic flatworms under aerobic (larval) and anaerobic (adult) conditions, which might be due to their different metabolic pathways (Soprunov, 1987; Moczoń, 2006; Wangckuk et al., 2023). As shown in our previous study (Poddubnaya et al., 2025), in a plerocercoid of a phyllobothriidean metacestode, genus *Clistobothrium* from the spiral intestine of *Chimaera monstrosa* (Holocephali) (anaerobic condition), the muscle cells contain glycogen and no lipid droplets.

Release of lipid droplets in adult parasitic worms

In flatworms, the excretion of metabolic waste products is thought to be accomplished by the epithelial lining of the gut, body wall via exocytosis of vesicles and protonephridial system (Hertel, 1993). In the tapeworms, which lack a digestive system, there are only 2 methods of waste product excretion: via the surface tegument and the excretory system. However, few morphological observations have been made regarding lipid excretion in adult tapeworms. For example, Brand (1966) pointed out that mature proglottids of polyzoic cestodes detach from the strobila, thereby releasing accumulated fatty acids. Lipid droplets have been recorded in the lumen of excretory ducts in the polyzoic tapeworms *Hymenolepis, Echinococcus* and *Moniezia* (Shultz and Gvozdev, 1972) and in the monozoic *Khawia armeniaca* (Poddubnaya, 2003). To our knowledge, there is only 1 transmission electron microscopy record of the release of lipid droplets via the dorsal tegumental surface in adult males of the digenean *Schistosoma mansoni* (Haseeb et al., 1985). Herein, a significant number of lipid droplets were observed in the body of adult *C. brachycollis*, which leave the worm's body through the tegumental surface and excretory system. This is consistent with the statement that lipids are truly excretory products when found in the bladder of adult tapeworms (Soprunov, 1987; Komuniecki and Harris, 1995; Wangckuk et al., 2023). Lipid droplets pass through the tegumental cytoplasmic processes into the distal cytoplasmic layer, which was documented in the current study for *C. brachycollis* and previously mentioned for *C. laticeps* (Richards and Arme, 1981). Our investigation showed that, in *C. brachycollis,* the lipid droplet was surrounded by an electron-lucent sac when they located in the distal tegumental cytoplasm. Lipid droplets are not membrane-bound substances, and their release outside the organism requires the droplets to be carried in a membrane-bound sac for release at the host–parasite interface. Our study confirms the involvement of electron-lucent tegumental vesicles in the formation of membrane-bound sacs through the accumulation and fusion of vesicles around lipid droplets.

Most adult trematodes release lipid droplets via excretory pore (Erasmus, 1967; Mattison et al., 1992; Poddubnaya et al., 2024). For adult tapeworms, there is a lack of ultrastructural studies concerning the detailed structure of the excretory bladder and the release of waste products through the excretory pore. Nevertheless, for larval tapeworms, some ultrastructural data exist on the excretory bladder of encapsulated plerocercoid stage of the diphyllobothriidean tapeworm, *Pyramicocephalus phocarum* (Mustafina and Biserova, 2022). The current study demonstrates that, in *C. brachycollis*, the syncytial epithelial lining of both the distal and proximal bladder parts is a derivative of the tegumental distal cytoplasm of the posterior body surface. Variations in the structural organization of the distal and proximal bladder parts of *C. brachycollis* were observed with respect to their luminal microtriches, and the presence of a folded epithelial lining elevated by large cytoplasmic protrusions in the proximal bladder. In *C. brachycollis*, abundant

https://doi.org/10.1017/S0031182026101930 Published online by Cambridge University Press

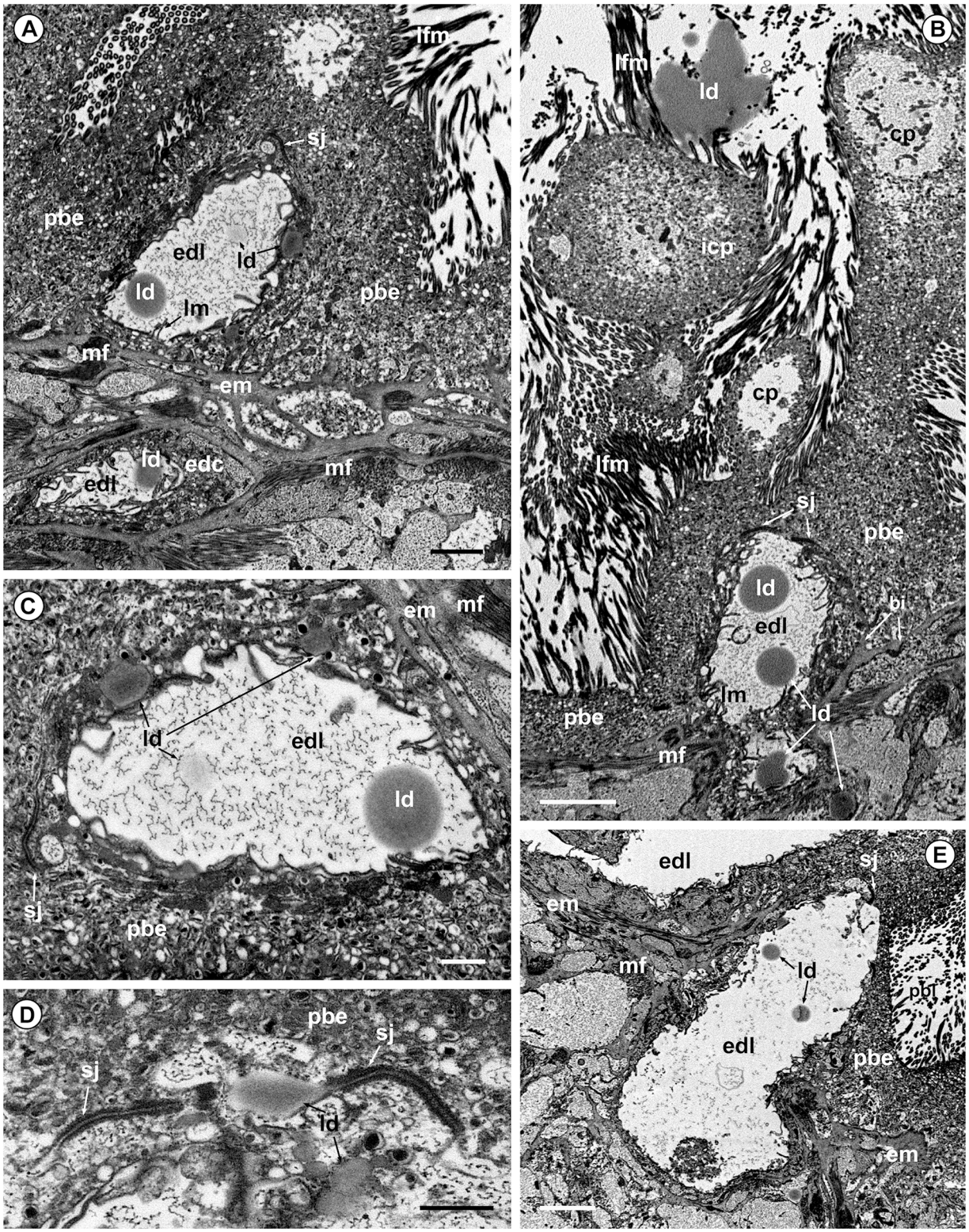

Figure 5. Release of lipid droplets into the proximal bladder lumen accomplished by the excretory ducts of *C. brachycollis*. (A) Proximal excretory bladder showing 2 portions of the excretory duct situated within and underneath the bladder epithelium. Scale bar = 1 µm. (B) Proximal bladder epithelium penetrated by an excretory duct with lipids within its lumen; note the isolated cytoplasmic protrusion and lipid droplets in the bladder lumen. Scale bar = 2 µm. (C) Excretory duct within the bladder epithelium showing lipid droplets within the duct epithelium and lumen; note the septate junction. Scale bar = 0.5 µm. (D) Septate junction connecting the duct and bladder epithelial plasma membranes; note the presence of lipid droplets. Scale bar = 0.5 µm. (E) Excretory duct penetrating bladder epithelium. Abbreviations: cp, cytoplasmic protrusion; edc, epithelial duct cytoplasm; edl, excretory duct lumen; em, extracellular basal matrix; icp, isolated cytoplasmic protrusion; ld, lipid droplets; lfm, long filamentous microtriches; lm, luminal lamellae of the excretory duct; mf, muscle fibres; n, nucleus; pbe, proximal bladder epithelium; sj, septate junction.

https://doi.org/10.1017/S0031182026101930 Published online by Cambridge University Press

lipid droplets are released into the proximal bladder lumen via 10 collecting descending excretory ducts. The Caryophyllidean species have a specific number (6–12) of interconnected longitudinal descending excretory ducts that directly release into the excretory bladder (Mackiewicz, 1972). The lack of available literature on the ultrastructural organization of the excretory bladder in adult tapeworms does not allow us to assess the degree of bladder morphological variability in cestodes, as has been documented for digeneans (Poddubnaya et al., 2024).

Comments on tapeworm storage lipid droplets

In adult *C. brachycollis*, lipid droplets were observed in cyrtocytes, in the cytoplasm of excretory cell bodies, in the epithelial linings of the excretory ducts and bladder, and within the excretory lumens. There is a lack of data on the presence of lipid droplets within cyrtocytes in tapeworms, where lipid droplets fill the area between the ciliary tuft and the cytoplasmic cord. We presume that these cyrtocytes are subject to subsequent apoptosis in *C. brachycollis*. The epithelial wall of the excretory ducts of digenean discharges lipid droplets into the lumen (Rohde, 1989; Mattison et al., 1992; Poddubnaya et al., 2024); the same finding was encountered here for *C. brachycollis*. In mature monozoic cestodes (e.g. *C. brachycollis*) and gravid proglottids of polyzoic cestodes, the sarcoplasmic processes are replete with lipid droplets (Shultz and Gvozdev, 1972; Biswal et al., 2014). Since the life span of most caryophyllidean tapeworms in their vertebrate hosts varies from 3 to 6 months, during which the adult worms commence egg production, the eggs subsequently occupy the greater part of worm's body, and the last step is the worm's destruction (Mackiewicz, 1972). Based on the records mentioned above and the results of current investigation, we suggest that the early larval stages of the tapeworm's development contain glycogen and lack storage lipids, regardless of the larval habitat, be it aerobic or anaerobic conditions.

It should also be noted that in biochemical reports on the quantity of lipids in adult tapeworms, the total amount of lipids was considered without distinction between excretory lipids (storage muscle cells and excretory system) and the lipids of the vitelline cells and eggs (Mondal et al., 2016; Yuskiv and Yuskiv, 2020; Bhogil et al., 2022; Phadke, 2024). It is reasonable to emphasize that the site of the formation of the tapeworm eggs is the ootype and the uterus, where the eggshell is formed around oocyte-vitelline cells complex with participation of the vitelline globules (Colhoun et al., 1998; Poddubnaya et al., 2005; Młocicki et al., 2010). Lipids of the muscle cells do not participate in the formation of the eggs, as it was documented in a number of biochemical papers (Mondal et al., 2016; Wangckuk et al., 2023). In the future, with the development of metabolomics methods, it is hoped to gain more data on a large number of different metabolites, including lipids, which are found in the excretory-secretory products of parasitic flatworms (Wangchuk et al., 2019, 2023).

Conclusion

The present data provide the first ultrastructural evidence of the lipid excretion via tegument and excretory system in adult tapeworm besides details on fine structure of the excretory bladder of the genus *Caryophyllaeus*. The study expands the morphological data on the fate of lipid droplets accumulating in parenchymal muscle cells in the tapeworms.

Acknowledgements. The authors are indebted to the staff of the Centre of Electron Microscopy, Institute for Biology of Inland Waters, Russian Academy of Sciences, for technical assistance with the scanning electron microscopy and transmission electron microscopy investigations. We thank Dr E. Franchella of the University of Ferrara for the technical assistance and Dr C. Holland from Trinity College Dublin for English correction of the MS. This research was carried out within the framework of the topic 'Morphology, physiology, and diversity of parasites of organisms of continental aquatic ecosystems', registration No. 124032500018–8, for Larisa Poddubnaya.

Author contributions. LGP: Conceptualization, investigation, data curation, writing – original draft and funding acquisition. ML: Methodology. GI: Methodology and investigation. AC: Methodology. BSD: Data curation and funding acquisition.

Financial support. This work was supported by grants for the project 'NaturBosnia' (Italian Agency for Development Cooperation) to M. Lorenzoni (University of Perugia) and from grants of the University of Ferrara to B. Sayyaf Dezfuli (FAR 2024).

Competing interests. The authors declare that they have no competing financial interests or personal relationships that may have influenced the work reported in this study.

Ethical standards. No fish were sacrificed or made to suffer because of this research activity since the digestive tracts came from eviscerated specimens caught for food purposes. Based on the actual laws of Italy, this type of organ collection does not require approval by the University of Animal Care Committee.

References

Alvite G and Esteves A (2012) Lipid binding proteins from parasitic Platyhelminthes. *Frontiers in Physiology* **3**, 363. https://doi.org/10.3389/fphys.2012.00363.

Bhogil A, Borde S and Thosar A (2022) Study of biochemical components of cestode parasites from *Capra hircus* (L) in Solapur District, India. *Uttar Pradesh Journal of Zoology* **43**, 74–77.

Biswal D, Nandi AP and Chatterjee S (2014) Biochemical and molecular characterization of the Cyclophyllidean cestode, *Cotugnia cuneata* (Meggit, 1924), an endoparasite of domestic pigeons, Columbia livia domestica. *Journal of Parasitic Diseases* **38**, 106–110. https://doi.org/10.1007/s12639-012-0203-3.

Brand T (1966) *Biochemistry of Parasites*. New York & London: Academic Press.

Bruňanaská M, Mackiewicz JS, Młocicki D, Świderski Z and Nebesářová J (2012) Early intrauterine embryonic development in *Khawia sinensis* Hsü, 1935 (Cestoda, Caryophyllidea, Lytocestidae), an invasive tapeworm of carp (*Cyprinus carpio*): An ultrastructural study. *Parasitology Research* **110**, 1009–1017.

Colhoun LM, Fairweather I and Brennan GP (1998) Observations on the mechanism of eggshell formation in the liver fluke, *Fasciopla hepatica*. *Parasitology* **116**, 555–567. https://doi.org/10.1017/s0031182098002662.

Conn DB (1993) The biology of flatworms (Platyhelminthes): Parenchyma cells and extracellular matrices. *Transactions of the American Microscopical Society* **112**, 241–261. https://doi.org/10.2307/3226561.

Conn DB and Etges FJ (1984) Fine structure and histochemistry of the parenchyma and uterine egg capsule of *Oochoristica anolis* (Cestoda: Linstowiidae). *Zeitschrift Für Parasitenkunde* **70**, 769–779. https://doi.org/10.1007/bf00927130.

Conn DB and Rocco LJ (1989) Fine structure of the cellular parenchyma and extracellular matrix of *Ophiotaenia loenbergii* (Cestoda: Proteocephalidea). *Acta Zoologica* **70**, 105–110. https://doi.org/10.1111/j1463-6395.1989.tb01059.x.

Erasmus DA (1967) Ultrastructural observations on the reserve bladder system of *Cyathocotyle bushiensis* Khan, 1962 (Trematoda: Strigeoidea) with special reference to lipid excretion. *Journal of Parasitology* **53**, 525–536. https://doi.org/10.2307/3276710.

Haseeb MA, Eveland LK, Fried B and Hayat MA (1985) Transmission electron microscopic observations on lipid release in *Schistosoma mansoni* maintained *in vitro*. *International Journal for Parasitology* **15**, 49–53. https://doi.org/10.1016/0020-7519(85)90100-6.

Hashimoto M and Hossain S (2018) Fatty acids: From membrane ingredients to signaling molecules. In *Biochemistry and Health Benefits of Fatty Acids*. Viduranga Waisundara, IntechOpen. http://dx.doi.org/10.5772/intechopen.80430.

Hertel L (1993) Excretion and osmoregulation in the flatworms. *Transactions of the American Microscopial Society* **112**, 10–17.

Humbe A, Jadhav S and Borde SN (2011) Biochemical studies of gastrointestinal cestode parasites in *Capra hircus* (L.) and *Ovis bharal* (L.) from Marathwada region. *International Multidisciplinary Research Journal* **1**, 8–10.

Izvekova GI (1997) The contents of proteins, carbohydrates and glucose transport in different parts of the strobila of cestode *Eubothrium rugosum*. *Parazitologiya* **31**, 90–96. (In Russian).

Janiszewska J (1953) *Caryophyllaeus brachycollis* n. sp. from cyprinid fishes. *Zoologica Poloniae* **6**, 57–68.

Jawale S, Fartade A and Borde S (2011) Biochemical studies of Caryophyllidean tapeworms in fresh water fish *Clarias batrachus*. *Recent Research in Science and Technology* **3**, 35–36.

Khawal R, Thosar A and Borde S (2020) Biochemical study of freshwater fish *Clarias batrachus* (L.) infected with cestode parasite, *Lytocestus*, sp. from Aurangabad District, India. *Global Journal for Research Analysis* **9**, 75–76. https://doi.org/10.36106/gjra.

Komuniecki R and Harris BG (1995) Carbohydrate and energy metabolism in helminths. In Marr JJ and Müller M (eds.), *Biochemistry and Molecular Biology of Parasites*. Harcurt Brace & Company, London & San Diego: Academic Press, pp. 49–67.

Mackiewicz JS (1972) Caryophyllidea (cestoidean): A review. *Experimental Parasitology* **31**, 417–512. https://doi.org/10.1016/0014-4894(72)90103-8.

Mattison RG, Hanna REB and Nizami WA (1992) Ultrastructure and histochemistry of the protonephridial system of juvenile *Paramphistomum epiclitum* and *Fischoederius elongates* (Paramphitomidae: Digenea) during migration in Indian ruminants. *International Journal for Parasitology* **22**, 1105–1115. https://doi.org/10.1016/0020-7519(92)90030-O.

Młocicki D, Świderski Z and Conn DB (2010) Ultrastructure of the early embryonic stages of *Corallobothrium fimbriatum* (Cestoda: Proteocephalidea). *Journal of Parasitology* **96**, 839–846. https://doi.org/10.1645/GE-24381.

Moczoń T (2006) Accumulation and utilization of lipids during the development of *Hymenolepis diminuta* cysticercoids. *Acta Parasitologica* **51**, 152–155.

Mondal M, Kundu JK and Misra KK (2016) Variation in lipid and fatty acid uptake among nematode and cestode parasites and their host, domestic fowl: Host-parasite interaction. *Journal of Parasitic Diseases* **40**, 1494–1518.

Mustafina AR and Biserova NM (2022) Excretory system ultrastructure of diphyllobothriid tapeworm *Pyramicocephalus phocarum* (Cestoda) with cytochemical and functional implication. *Invertebrate Zoology* **19**,159–184. (In Russian). https://doi.org/10.15298/invertzool.19.2.05.

Nanware SS, Bhure DB and Habib MH (2012) Glycogen content in *Moniezia expansa* and its host intestine. *Indian Journal Applied Research* **4**, 651–652.

Phadke S (2024) Biochemical Changes in the intestine of goat infected with cestode parasites. *Indian Journal of Research* **13**, 37–38.

Poddubnaya LG (1995) Peculiarities of the integument genesis in procercoids of caryophyllidean cestodes. *Parazitologiya* **29**, 13–18. (In Russian).

Poddubnaya LG (2003) Polymerization related to size of monozoic cestodes (ultrastructural analysis). *Zoologicheskiy Zhurnal* **83**, 3–12. In Russian.

Poddubnaya LG, Hemmingsen W and MacKenzie K (2024) Comparative analysis of the cytoarchitecture of the excretory bladder of adult Digenea (Platyhelminthes) with consideration of the presence of mineralized excretory corpuscles in marine and freshwater adult worms. *Zoologischer Anzeiger* **309**, 28–36. https://doi.org/10.1016/j.jcz.2024.01.005.

Poddubnaya LG, Kuchta R and Scholz T (2025) First record of phyllobothriid metacestodes in *Chimaera monstrosa* (Holocephali) and *Oncophynchus gorbuscha* (Salmonidae): Novel insight into larval topography and ultrastructure. *Journal of Parasitology* **111**, 419–430. https://doi.org/10.1645/24-136.

Poddubnaya LG, Mackiewicz JS and Kuperman BI (2003) Ultrastructure of *Archigetes sieboldi* (Cestoda: Caryophyllidea): Relationship between progenesis, development and evolution. *Folia Parasitologica* **50**, 275–292. https://doi.org/10.14411/fp.2003.047.

Poddubnaya LG, Mackiewicz JS, Świderski Z, Bruňanaská M and Scholz T (2005) Fine structure of egg-forming complex ducts, eggshell formation and supporting neuronal plexus in progenetic *Diplocotyle olrikii* (Cestoda, Spathebothriidea). *Acta Parasitologica* **50**, 292–304.

Richards KS and Arme C (1981) The ultrastructure of the scolex-neck syncytium, neck cells and frontal gland cells of *Caryophyllaeus laticeps* (Caryophyllidea: Cestoda). *Parasitology* **83**, 477–487. https://doi.org/10.1017/S003118200008046X.

Ritler D, Rufener R, Li JV, Kämpfer U, Müller J, Bühr C, Schürch S and Lundström-Stadelmann B (2019) In vitro metabolomic footprint of the *Echinococcus multilocularis* metacestode. *Scientific Reports* **9**(19438), 1–13.

Rohde K (1989) Ultrastructure of the protonephridial system of *Lobatostoma manteri* (Trematoda, Aspidogastrea). *Journal of Submicroscopic Cytology and Pathology* **21**, 599–610.

Saraf PS and Katyayani R (2020) Biochemical estimation of *Senga* sp. in fresh water fish *Mastacembelus armatus* from Paithan District. Aurangabad, India. *International Journal of Scientific Research* **9**, 24–25.

Sayyaf Dezfuli B, Lorenzoni M, Carosi A, Bosi G, Franchella E and Poddubnaya LG (2024) Glandular cell products in adult cestodes: A new tale of tapeworm interaction with fish innate immune response. *International Journal for Parasitology: Parasites and Wildlife* **25**, 100991. https://doi.org/10.1016/j.ijppaw.2024.100991.

Shultz PC and Gvozdev EB (1972) *Biology of Helminths*. Vol. II, Nauka: Moscow published house. p. 515.

Smyth JD and McManus DP (1989) *The Physiology and Biochemistry of Cestodes*. Cambridge, UK: Cambridge University Press. p. 412.

Soprunov FF (1987) *Molecular Basis of Parasitism*, Nauka: Moscow published house. p. 223.

Świderski Z, Bruňanská M, Poddubnaya LG and Mackiewicz JS (2004) Cytochemical and ultrastructural study on vitellogenesis in caryophyllidean cestode *Khawia armeniaca* (Cholodkovski, 1915). *Acta Parasitologica* **49**, 16–24.

Świderski Z and Mackiewicz JS (1976) Electron microscope study of vitellogenesis in *Glaridacris catostomi* (Cestoidea: Caryophyllidea). *International Journal for Parasitology* **6**, 61–73. https://doi.org/10.1016/0020-7519(76)90011-4.

Świderski Z, Młocicki D, Mackiewicz JS, Miquel J, Ibraheem MH and Bruňanská M (2009) Ultrastructure and cytochemistry of vitellogenesis in *Wenyonia virilis* Woodland, 1923 (Cestoda, Caryophyllidea). *Acta Parasitologica* **54**, 131–142.

Świderski Z and Xylander WER (2000) Vitellocytes and vitellogenesis in cestodes in relation to embryonic development, egg production and life cycle. *International Journal for Parasitology* **20**, 805–817. https://doi.org/10.1016/S0020-7519(00)00066-7.

Wangchuk P, Constantinoiu C, Eichenberger RM, Field M and Loukas A (2019) Characterization of tapeworm metabolites and their reported biological activities. *Molecules* **24**, 1480.

Wangckuk P, Yeshi K and Loukas A (2023) Metabolomics and lipidomics studies of parasitic helminths: Molecular diversity and identification levels achieved by using different characterization tools. *Metabolomics* **19**, 63. https://doi.org/10.1007/s11306-023-02019-5.

Yeshi K, Ruscher R, Loukas A and Wangchuk P (2022) Immunomodulatory and biological properties of helminth-derived small molecules: Potential applications in diagnostics and therapeutics. *Frontiers in Parasitology* **1**, 984152. https://doi.org/10.3389/fpara.2022.984152.

Yuskiv LL and Yuskiv ID (2020) The lipid metabolism in carp during invasion by the tapeworm *Bothriocephalus acheilognathi*. *Regulatory Mechanisms in Biosystems* **11**, 214–219. https://doi.org/10.15421/022031.

https://doi.org/10.1017/S0031182026101930 Published online by Cambridge University Press